JOURNAL OF MATERIALS SCIENCE 38 (2003) 2809–2814

Reaction-induced phase separation in an epoxy/low molecular weight solvent system

E. SOULÉ, M. GARCÍA DE LA MATA, J. BORRAJO, P. A. OYANGUREN, M. J. GALANTE*
Institute of Materials Science and Technology (INTEMA), University of Mar del Plata and National Research Council (CONICET), J. B. Justo 4302, 7600 Mar del Plata, Argentina

Blends based on a stoichiometric mixture of diglycidyl ether of bisphenol A (DGEBA) and 2,2′-bis(4-amino-cyclohexyl)methane (ACHM) and cyclohexane as low molecular weight solvent were studied. The polymerization kinetics data experimentally obtained at different temperatures (30–60°C) were accurate fitted using a mechanistic model. The effect of the solvent over the polymerization rate was analyzed. No influence of the presence of the solvent was found up to 20 wt% of cyclohexane in the sample. The thermodynamic analysis using Flory-Huggins model allowed determination of the initial miscibility of binary blends containing DGEBA/cyclohexane and pseudo-binary mixtures of DGEBA/ACHM/cyclohexane. The presence of ACHM increases the DGEBA/cyclohexane initial solubility. The reaction-induced phase separation was described using a conversion-composition transformation phase diagram. It indicates that phase separation takes place by a nucleation and growth (NG) mechanism. The appropriate selection of composition of the blend and polymerization conditions led to final materials with a desired closed cell porous morphology.

1. Introduction

Porous polymers have found many useful applications: foams, membranes, filters, chromatography supports, etc. Therefore, an important fact to consider in their preparation, depending on their possible use, is the control of porosity (open or closed cells, porosity size and size distribution).

Kiefer *et al.* [1–3] have successfully developed a new technology that allowed them to synthesize porous materials by way of a chemical induced phase separation process. The control of the morphology requires a knowledge of the phase diagram, the reaction kinetics and thermodynamics of phase separation. As is well known [4] the competition between polymerization and phase separation leads to a nucleation and growth or spinodal demixing mechanism. Independent of the mechanism by which phase separation is produced, final morphologies depend also on the location of the trajectory in the conversion-vs.-composition transformation diagram. If the modifier volume fraction (ϕ_o) is located in the off-critical region, the final morphology will consist of a dispersion of solvent-rich particles in a thermoset-rich matrix or either in a dispersion of thermoset-rich particles in a solvent-rich phase. In a composition region close to the critical point a variety of morphologies may be developed.

Thus, taking all these points in consideration, the main objective of this work is to analyze the composition, thermodynamics and kinetics factors that produce a porous morphology during the curing of an epoxy resin in the presence of a low molecular weight solvent.

2. Experimental

The epoxy resin used was a commercial diglycidyl ether of bisphenol A (DGEBA, MY 790 Ciba-Geigy). It had a weight per epoxy group, WPE = 177 g mol^{-1} as determined by acid titration. The amine, 2,2′-bis(4-amino-cyclohexyl)methane (ACHM, Aldrich), was used as received. The selected low molecular weight solvent was cyclohexane.

Blends containing stoichiometric amounts of diepoxide and diamine and variable concentrations of solvent were prepared according to the following procedure. The epoxy and the amine were first dissolved at approximately 40°C. Then, the solvent was added at room temperature under gentle stirring until a homogeneous solution was obtained. The solution was transferred into a glass tube and placed in liquid air to avoid solvent evaporation, following the procedure proposed by Kiefer *et al.* [1]. After sealing under vacuum, the sample was allowed to return to room temperature. The blends were cured in an oil bath kept at constant temperature (20–60°C) during the time required to reach maximum conversion. After that, the tubes were opened and heated at 180°C for 48 h in a vacuum oven, in order to evaporate the solvent and complete the polymerization reaction.

*Author to whom all correspondence should be addressed.

0022–2461

Near-infrared spectroscopy (NIR) was used to follow the polymerization kinetics up to 60°C, measuring the variation of the height of the absorption band at 4530 cm^{-1} (epoxy group) relative to the height of the band at 4621 cm^{-1} (phenyl group) [5]. An FTIR Mattson, Genesis II was employed, provided with a heated transmission cell with quartz windows and a programmable temperature controller.

A Shimadzu DSC-50 differential scanning calorimeter (DSC) was used at 10°C min^{-1} under nitrogen, to determine the reaction heat for the initial formulation in a dynamic scan (ΔH_{max}) and its glass transition temperature (T_g).

Phase separation temperatures and times were determined by visual inspection of the samples. A neat and reproducible transition from a clear to a milky state was taken as the cloud-point.

To obtain gelation times a set of tubes was placed in an oil bath at constant temperature. The tubes were extracted at different times and chilled in iced-water to stop the reaction. Then, tetrahydrofuran (THF) was added. Gelation was ascribed to the time in which an incipient insoluble fraction appeared.

Plaques were fractured with a razor blade at room temperature coated with a fine gold layer and observed by scanning electron microscopy (SEM) on a Jeol JSM 35 CF device.

3. Results and discussion

3.1. Cure kinetics

The total reaction heat determined by differential scanning calorimetry, was 95.3 kJ/mol for the neat system and 97.3 kJ/mol for the sample with solvent. These values were in good agreement with the data reported in literature for these kind of chemical systems (epoxy-amine). The glass transition temperature, obtained in a second scan, was approximately 130°C. No variation of this value was observed, within the experimental error, for the samples with solvent. This fact indicates that, if there is some, only a few traces of cyclohexane remains in the epoxy matrix after phase separation.

The polymerization kinetics were evaluated using the mechanistic model proposed by Girard-Reydet *et al.* [6]. The epoxy-amine reaction is well known [7–14]. The first step involves the reaction between the primary amine hydrogen and epoxy. This reaction is followed by the reaction of the secondary amine generated with another epoxy group. The reactivities of the primary and secondary groups may be different. In the case of aliphatic amines the substitution effect is low and the ratio of reactivities $N = k_2/k_1$ could be taken equal to one [15].

An etherification step may take place depending on temperature and basicity of the diamine. When aliphatic amines are used this reaction can be neglected [6, 7, 16–18]. Two mechanisms compete during the polymerization reaction. The hydroxyl groups catalyze one and the other is a noncatalytic mechanism. Considering those epoxy-amine reaction paths, the following kinetics equations may be written:

$$-\frac{de}{dt} = [k_1' + k_1(OH)]e(a_1 + Na_2) \quad (1)$$

$$-\frac{da_1}{dt} = [k_1' + k_1(OH)]2ea_1 \quad (2)$$

$$\frac{da_2}{dt} = [k_1' + k_1(OH)]e(a_1 - Na_2) \quad (3)$$

$$\frac{dOH}{dt} = [k_1' + k_1(OH)]e(a_1 + Na_2) \quad (4)$$

where e is the concentration of epoxy equivalents, a_1 is the concentration of primary amine hydrogens, a_2 is the concentration of secondary amine hydrogens, and [OH] is the concentration of hydroxyl groups. In adittion, k_1 is the specific rate constant for the catalyzed reaction, k_1' is the specific rate constant for the non catalyzed reaction.

Assuming that $x = (e_0 - e)/e_0$, $a = a_1/e_0$, $K_1' = k_1'e_0^2$, $K_1 = k_1e_0$, and defining the relationship between amine and epoxy concentration, the chemical constants for a stoichiometric system may be expressed by:

$$\frac{dx}{dt} = \frac{(1-x)}{2-N}\left\{K_1' + K_1\left[1 + \frac{(OH)_0}{e_0} - \frac{1}{2-N}[(1-N)a + a^{N/2}]\right]\right\} * [2(1-N)a + Na^{N/2}] \quad (5)$$

$$x = \frac{1}{2-N}((1-a)(1-N) + (1-a^{N/2})) \quad (6)$$

$$\frac{da}{dt} = 2a(1-x)\left\{K_1' + K_1\left[1 + \frac{(OH)_0}{e_0} - \frac{1}{2-N}[(1-N)a + a^{N/2}]\right]\right\} \quad (7)$$

Conversion vs. time curves were obtained at constant temperature using NIR for formulations with and without solvent. The chemical rate constants were determined using the experimental results in the range 30–60°C. The theoretical results obtained using the kinetic model appear plotted in Fig. 1 together with the experimental data, and as is shown, accurate fit those values. The activation energies for the autocatalytic and non-catalytic mechanism were determined taking into account an Arrhenius temperature dependence. The correspondent values of the chemical constant rates were:

$$A1 = 1.17 \times 10^8\ min^{-1} \quad E1 = 60.9\ kJ/mol \quad (8)$$

$$A1' = 1.34 \times 10^{19}\ min^{-1} \quad E1' = 128.9\ kJ/mol \quad (9)$$

The activation energy for the catalyzed reaction compares reasonably well with values reported in literature [19–22] for similar systems. The influence of cyclohexane on the epoxy-amine cure kinetics was also analyzed. Fig. 2 shows that there is no appreciable modification of the polymerization rate in presence of up to 20 wt% of solvent over the interval of temperatures studied.

The gelation conversion determined by solubility in THF at different temperatures (40, 50 and 60°C), $x_{gel} = 0.57 \pm 0.03$, agrees well with the theoretical

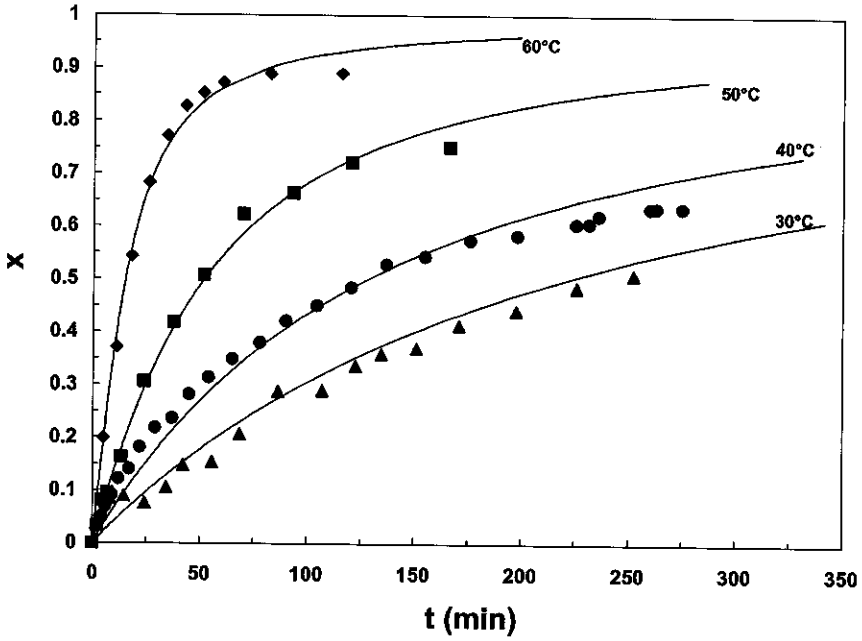

Figure 1 Conversion vs. time curves for the epoxy-amine neat system at different polymerization temperatures. The full lines indicate the kinetics model.

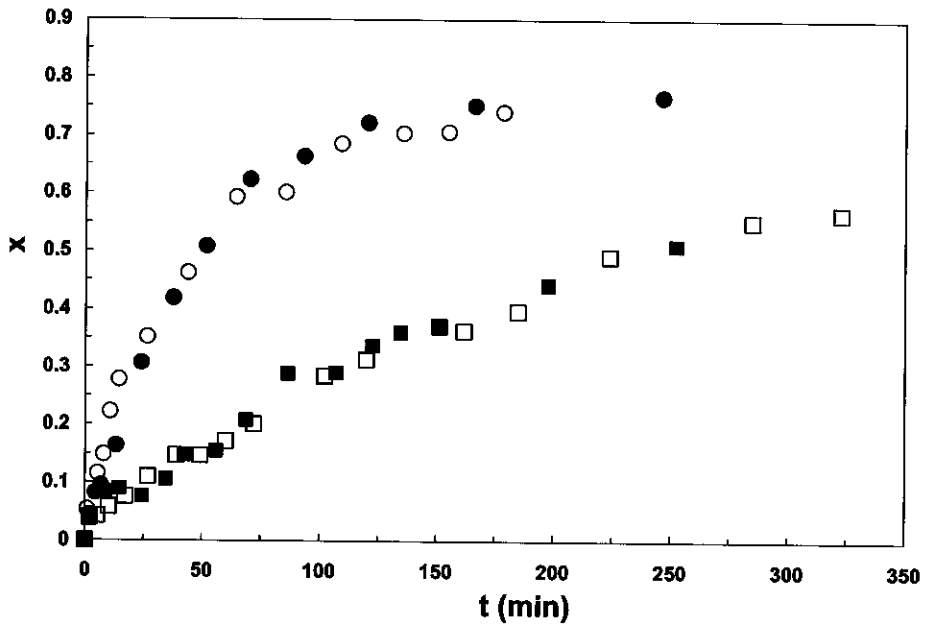

Figure 2 Conversion vs. time curves for the neat epoxy-amine system and in the presence of 20 wt% of cyclohexane at different curing temperatures (30°C, 50°C) (open symbols correspond to modified systems).

value calculated for and epoxy-diamine reaction ($x_{gel} = 0.57$).

3.2. Non reactive system phase diagrams

The phase separation behavior was experimentally studied. The obtained curves were theoretically analyzed and the interaction parameter determined using the Flory-Huggins lattice model. The corresponding expression for the Gibbs free energy of the system is given by:

$$\Delta G/RT = \phi_s \ln \phi_s + \phi_E/Z \ln \phi_E + \chi \phi_s \phi_E \quad (10)$$

where R is the gas constant, and ϕ_E and ϕ_S are the volume fractions of epoxy and cyclohexane, respectively. A unit cell is defined with a molar volume V_r (reference volume), selected as the molar volume of the solvent cyclohexane (V_s) the smallest species present in the system ($Z = V_E/V_r$). The cloud point data (CPC) for DGEBA/cyclohexane binary system are shown in Fig. 3. The curve also gives the values fitted using the thermodynamic model with a χ (T) relationship given by the following equation:

$$\chi = -0.567 + 683.9/T \text{ (K)} \quad (11)$$

This blend behaves as a typical system with an upper critical solution temperature (UCST) (i.e., miscibility increases with temperature) with a χ value decreasing with temperature. The influence of the addition of the

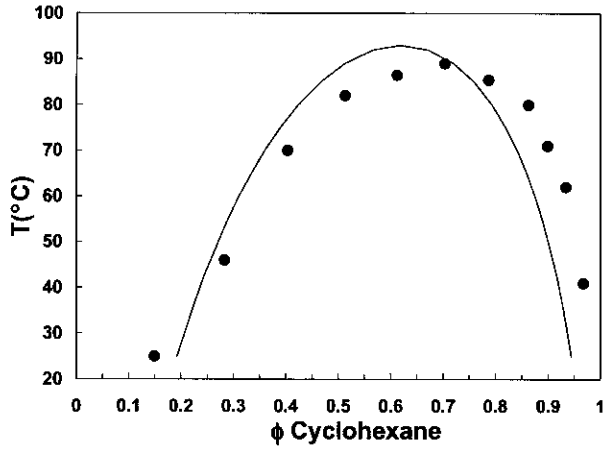

Figure 3 Cloud-point temperature vs. volumetric fraction of cyclohexane in DGEBA/cyclohexane blends. Full line corresponds to calculated CPC.

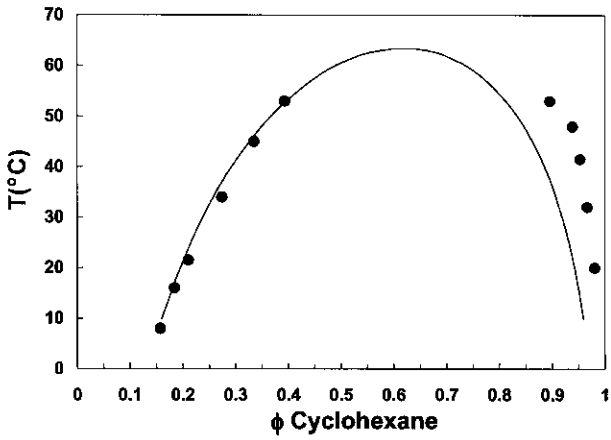

Figure 4 Cloud-point temperature vs. volumetric fraction of cyclohexane in DGEBA/ACHM/cyclohexane blends before reaction. Full line corresponds to calculated CPC.

diamine over the phase separation curve was also considered (see Fig. 4). The full line in Fig. 4 shows the fitting of the cloud point curve by the model. The corresponding value for the interaction parameter results in:

$$\chi = -1.506 + 953/T\ (\mathrm{K}) \qquad (12)$$

The presence of the amine actually modifies the binary phase diagram. ACHM increases the miscibility of the pair DGEBA/cyclohexane.

3.3. Phase separation during chemical reaction

Phase separation times obtained by visual inspection in the 30–50°C interval, were converted to cloud point conversions employing the kinetics data for DGEBA/ACHM. It was assumed that the addition of solvent does not produce any change in the reaction kinetics as it was shown in Fig. 2. The restriction in the interval of temperature analyzed was because at lower temperatures the system is initially phase separated for blends containing more than 20 wt% of cyclohexane (as it was shown in Fig. 4), and if the polymerization temperature becomes high the increase in reaction rate makes cloud point conversions difficult to determine.

The study of the phase separation process was performed taking conversion (x) as an independent variable [23, 24]. In this case the mixture contains two components, polymer and solvent, and the thermodynamic equations could be solved considering the polydispersity of the thermosetting polymer [25–28]. We limited the analysis to the pre-gel stage where the phase separation process takes place.

The molar concentration of generic $E_{m,n}$ species, containing m ACHM and n DGEBA molecules, at an overall conversion x, is given by the Stockmayer distribution function [29, 30].

$$E_{m,n} = [\mathrm{ACHM}]o[4(3m)!x^{m+n-1}(1-x)^{2m+2}]/ [m!(3m-n+1)!(n-m+1)!] \qquad (13)$$

where $[\mathrm{ACHM}]o$ is the initial molar concentration of diamine in the mixture. The volume fraction of an $E_{m,n}$ species in the mixture, is given by:

$$\phi_{m,n} = E_{m,n}V_{m,n} = E_{m,n}[m(M_{\mathrm{ACHM}}/\rho_{\mathrm{ACHM}}) + n(M_{\mathrm{DGEBA}}/\rho_{\mathrm{DGEBA}})] \qquad (14)$$

$V_{m,n}$ is the molar volume of $E_{m,n}$ and ρ_i is the density of the component i in the mixture. Then, the free energy of mixing per mol of unit cell is:

$$\Delta G/RT = \phi_s \ln \phi_s + \Sigma\Sigma(\phi_{m,n})/Z_{m,n} \ln \phi_{m,n} + \chi\phi_s\phi_2 \qquad (15)$$

where $Z_{m,n} = V_{m,n}/V_r$, $\phi_2 = \Sigma\Sigma\,\phi_{m,n}$, and χ is a pseudobinary interaction parameter between cyclohexane and $E_{m,n}$ species. The variation of the chemical structure of starting monomers and oligomers is reflected by an overall dependence of χ with conversion x:

$$\chi = -1.506 + 953/T\ (\mathrm{K}) - 0.7595x + 0.499x^2 \qquad (16)$$

The interaction parameter decreases with conversion, indicating that oligomeric species are more compatible with cyclohexane than the initial blend epoxy-amine. Similar behavior was observed for an epoxy-diamine system modified with polyetherimide [31] and rubber-modified polycyanates [32]. The occurrence of the phase separation could be explain by considering the decrease in the entropic contribution, due to the increase in the average molar size of oligomeric species, over the enthalpic contribution on the free energy of mixing.

The reaction-induced phase separation may be described using conversion-vs.-composition transformation diagrams at constant temperature. As an example, cloud point conversion (x_{cp}) vs. concentration of cyclohexane (ϕ_s) curves, at 40 and 50°C, appear plotted in Fig. 5. The continuous line represents the fitting provided by a Flory-Huggins model with an interaction parameter depending on temperature and conversion

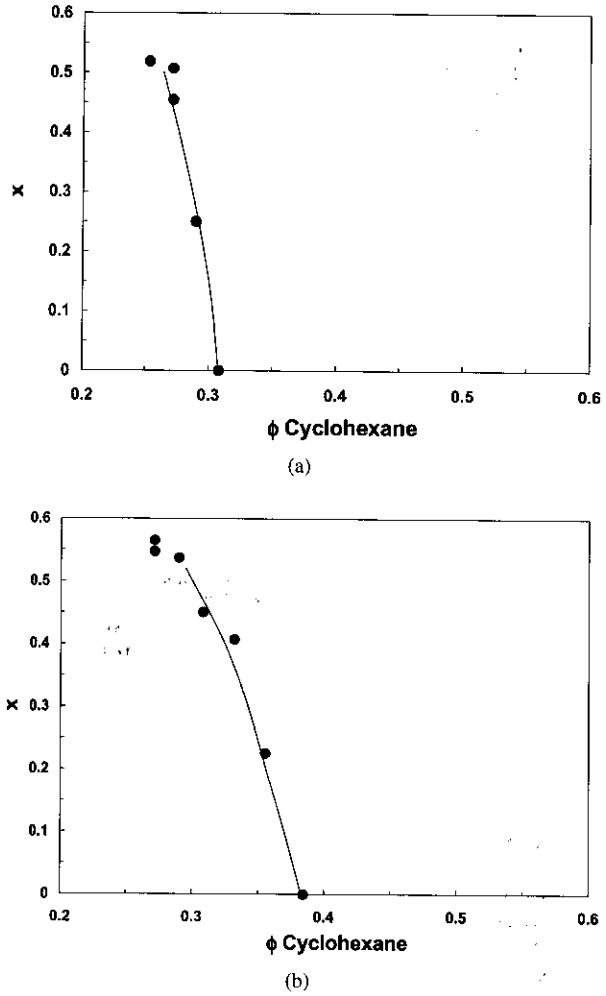

Figure 5 Cloud-point conversion as a function of volumetric fraction of cyclohexane in a mixture which undergoes polycondensation at different temperatures: (a) 40°C and (b) 50°C.

(Equation 16). They show that as is typical for an upper critical dissolution temperature system, x_{cp} shifts upward with increasing polymerization temperature.

The experimental values obtained in the low content of cyclohexane zone (where the morphological analysis was developed), accurate fitted the binodal curve. It indicates that phase separation would take place in the metastable region by a nucleation and growth (NG) mechanism.

3.4. Morphologies generated

In order to obtain porous materials, samples containing between 15 and 25 wt% of cyclohexane (composition located in the off-critical region of the phase separation diagram, to the left of $\phi_{s,crit.}$) cured at constant temperature during the period of time necessary to reach maximum conversion, were postcured 48 hs under vacuum at 180°C. Following this treatment, the polymerization reaction was completed and the solvent evaporated. The generated morphologies were analyzed using SEM. Figs 6 and 7 show that the expected closed cell morphology with narrow pore size distribution is attained. In addition, the influence of solvent concentration and curing temperature over the average size and concentration of the dispersed domains was studied. For samples

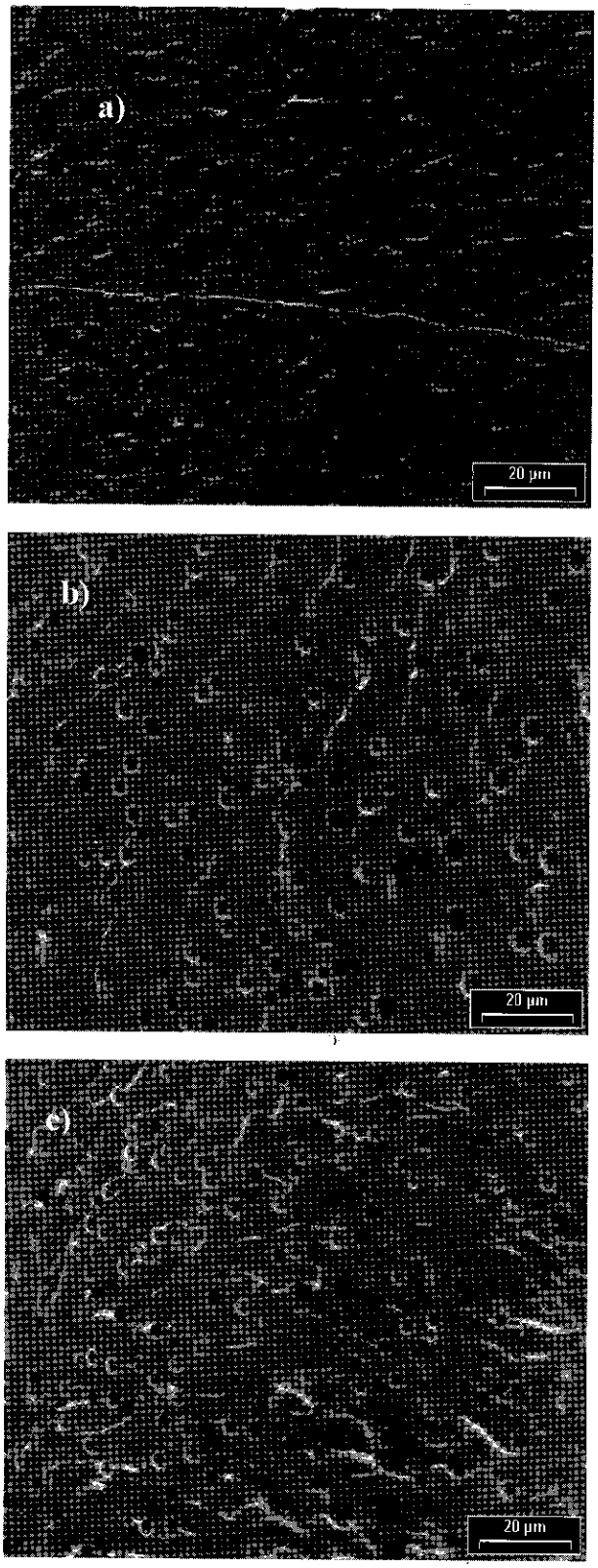

Figure 6 SEM micrographs of blends polymerized at 40°C containing 15, 20 and 25 wt% of cyclohexane.

cured at 40°C, an increase in the solvent content leads to an increment in the mean diameter of the particles from values close to 1 μm to approximately 2.5 μm (Fig. 6). A similar effect is found for a sample with 20 wt% of cyclohexane when polymerization temperature is increased, a structure with larger diameter particles is developed as is seen in Fig. 7.

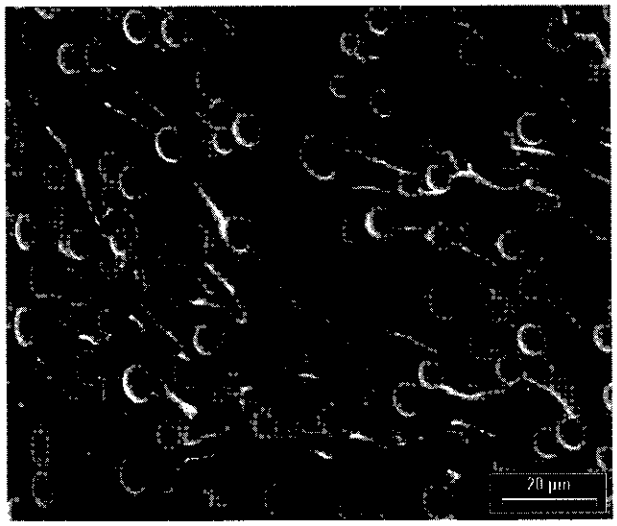

Figure 7 SEM micrograph of a blend containing 20 wt% of cyclohexane polymerized at 30°C.

4. Conclusions

The reaction-induced phase separation during the cure of an epoxy-diamine system in presence of a low molecular weight solvent, cyclohexane, was carefully analyzed. The polymerization kinetics were evaluated using a mechanistic model. An accurate fitting of experimental values was obtained showing that there is no influence of the presence of the solvent over the reaction rate up to 20 wt% of cyclohexane in the initial blend.

It was observed that the epoxy-solvent system behaves as typical upper critical solution temperature blend with an interaction parameter decreasing with temperature. It was also found that ACHM modifies the binary phase diagram increasing the miscibility of the pair DGEBA/cyclohexane. Phase separation during the chemical reaction was investigated and a simple thermodynamic model was used to predict cloud point conversion at different temperatures and solvent concentrations. It allowed us to conclude that phase separation takes place by the way of a nucleation and growth mechanism.

With the help of these studies, the appropriate selection of polymerization temperature and solvent concentration permitted us to obtain final materials with the desired closed cell morphology with narrow pore size distribution. Then, this work opens the possibility of choosing the conditions to generate materials with different morphologies and associated properties.

Acknowledgements

The financial support of CONICET, ANPCyT, Fundación Antorchas and University of Mar del Plata (Argentina) is gratefully acknowledged.

References

1. J. KIEFER, J. G. HILBORN and J. L. HEDRICK, *Polymer* **47**(25) (1996) 5715.
2. J. KIEFER, J. G. HILBORN, J. A. MANSON, Y. LETERRIER and J. L. HEDRICK, *Macromolecules* **29** (1996) 4158.
3. J. KIEFER, H. J. CHA, D. Y. YOON, J. C. HEDRICK, J. G. HILBORN and J. L. HEDRICK, *ibid.* **29** (1996) 8546.
4. R. J. J. WILLIAMS, B. A. ROZENBERG and J. P. PASCAULT, *Adv. Polym. Sci.* **128** (1997) 95.
5. N. POISSON, G. LACHENAL and H. SAUTEREAU, *Vib. Spectrosc.* **12** (1996) 237.
6. E. GIRARD-REYDET, C. C. RICCARDI, H. SAUTEREAU and J. P. PASCAULT, *Macromolecules* **28** (1995) 7599.
7. K. HORIE, H. HIURA, M. SAUVADA, I. MIKA and H. KAMBE, *J. Polym. Sci., Polym. Chem. Ed.* **8** (1970) 1357.
8. K. DUSEK, M. ILAVSKY and S. LUNAK, *J. Polym. Sci., Polym. Symp.* **53** (1975) 29.
9. S. LUNAK and K. DUSEK, *ibid.* **53** (1975) 45.
10. J. J. CHARLESWORTH, *ibid.* **18** (1980) 621.
11. B. A. ROZENBERG, "Epoxy Resins and Composites-I," Vol. 72 (Springer, Berlin, Adv. Polym. Sci., 1985) p. 113.
12. A. SABRA, T. M. LAM, J. P. PASCAULT, M. F. GRENIER-LOUSTALOT and P. GRENIER, *Polymer* **28** (1987) 1030.
13. C. S. P. SEUNG, E. PYMM and H. SUN, *Macromolecules* **19** (1986) 2922.
14. C. C. RICCARDI, H. E. ADABBO and R. J. J. WILLIAMS, *J. Appl. Polym. Sci.* **29** (1984) 2481.
15. K. DUSEK, *Adv. Polym. Sci.* **78** (1986) 1.
16. L. SCHECHTER, J. WYNSTRA and R. P. KURKJY, *Ind. Eng. Chem.* **48** (1956) 94.
17. L. A. O'NEILL and C. P. COLE, *J. Appl. Chem.* **6** (1956) 356.
18. H. DANNEMBERG, *Soc. Plast. Eng. Trans.* **3** (1963) 78.
19. D. VERCHÈRE, H. SAUTEREAU, J. P. PASCAULT, C. C. RICCARDI, S. M. MOSCHIAR and R. J. J. WILLIAMS, *Macromolecules* **23** (1990) 725.
20. G. J. WISANRAKKIT and K. GILLHAM, *J. Appl. Polym. Sci.* **41** (1990) 2885.
21. N. GALEGO, A. VAZQUEZ and R. J. J. WILLIAMS, *Polymer* **35** (1994) 857.
22. C. W. W. WISE and D. A. A. COOK GOODWIN, *ibid.* **38** (1997) 3251.
23. R. J. J. WILLIAMS, J. BORRAJO, H. E. ADABBO and A. J. ROJAS, in "Rubber-Modified Thermoset Resins; Adv. Chem. Ser." Vol. 208, edited by C. K. Riew and J. K. Gillham (American Chemical Society, Washington DC, 1984) p. 195.
24. A. VAZQUEZ, A. J. ROJAS, H. E. ADABBO, J. BORRAJO and R. J. J. WILLIAMS, *Polymer* **28** (1987) 1156.
25. C. C. RICCARDI, J. BORRAJO and R. J. J. WILLIAMS, *ibid.* **35** (1994) 5541.
26. N. CLARKE, T. C. B. MCLEISH and S. D. JENKINS, *Macromolecules* **28** (1995) 4650.
27. J. BORRAJO, C. C. RICCARDI, R. J. J. WILLIAMS, H. MASOOD SIDDIQI, M. DUMON and J. P. PASCAULT, *Polymer* **39** (1998) 845.
28. C. C. RICCARDI, J. BORRAJO, R. J. J. WILLIAMS, H. MASOOD SIDDIQI, M. DUMON and J. P. PASCAULT, *Macromolecules* **31** (1998) 1124.
29. W. H. STOCKMAYER, *J. Polym. Sci.* **9** (1952) 69.
30. *Idem., ibid.* **11** (1953) 424.
31. C. C. RICCARDI, J. BORRAJO, R. J. J. WILLIAMS, E. GIRARD-REYDET, H. SAUTEREAU and J. P. PASCAULT, *J. Polym. Sci., B: Polym. Phys.* **34** (1996) 349.
32. J. BORRAJO, C. C. RICCARDI, R. J. J. WILLIAMS, Z. Q. CAO and J. P. PASCAULT, *Polymer* **36** (1995) 3541.

Received 30 December 2002
and accepted 9 April 2003